Journal of Catalysis 264 (2009) 67–76

Contents lists available at ScienceDirect

Journal of Catalysis

journal homepage: www.elsevier.com/locate/jcat

Reactive oxygen on a Au/TiO_2 supported catalyst

M. Kotobuki, R. Leppelt [1], D.A. Hansgen [2], D. Widmann, R.J. Behm *

Institute of Surface Chemistry and Catalysis, University Ulm, D-89069 Ulm, Germany

ARTICLE INFO

Article history:
Received 7 January 2009
Revised 4 March 2009
Accepted 19 March 2009
Available online 25 April 2009

Keywords:
Au/TiO_2
CO oxidation
Oxygen storage capacity (OSC)
Temporal analysis of products (TAP)

ABSTRACT

We investigated the oxygen storage capacity (OSC) of Au/TiO_2 catalysts as well as its correlation with the activity for CO oxidation and in particular the influence of the Au particle size on these properties in kinetic measurements and in temporal analysis of products (TAP) reactor measurements. Catalysts with identical Au loading but different Au particle sizes were prepared by calcination of the same raw catalyst in air at different temperatures; the Au particle sizes were characterized by transmission electron microscopy and X-ray diffraction. TAP multi-pulse data indicate that oxygen stored on the catalyst surface reacts with CO; both the OSC and the activity for CO oxidation increase with decreasing Au particle size. From the small amount of removable oxygen, between 0.4 and 1.0% of the total surface oxygen of the support material, and its almost linear relation with the perimeter sites of the interface between the gold particles and the support, we suggest that the removable oxygen species are located at these interfacial perimeter sites. Furthermore, these oxygen species are shown to represent the active oxygen in the CO oxidation reaction under the present reaction conditions.

1. Introduction

Oxide-supported gold catalysts and in particular Au/TiO_2 catalysts are well known for their high activity for CO oxidation even at low temperatures [1–5]. Despite extensive efforts to unravel the reaction mechanism and the physical origin of their high activity on a molecular scale (for reviews see [4,5]), essential features of the reaction such as (i) the nature of the active site, (ii) the activation of oxygen and the nature of the active oxygen species, (iii) the effect of the Au particle size on the catalyst activity, and (iv) the role of the support and of metal-support interactions in the reaction and their influence on the catalytic activity are not yet resolved and are still under debate. For instance, while most groups agreed on small Au^0 nanoparticles as reaction dominating species (see, e.g., [4,5]), other groups proposed that cationic Au species play an essential role in the reaction [6–8]. Under-coordinated sites on the Au nanoparticles [9–11], support-induced strained Au [12], or 'perimeter sites' at the interface between Au nanoparticle and TiO_2 support [8,11,13–15] (or step sites at the perimeter [16]) were suggested as active sites. Furthermore, while there is a general agreement that CO is largely adsorbed on the Au nanoparticles (only for very low temperatures/high CO partial pressures CO is also adsorbed on the TiO_2 support), the activation of O_2 for the reaction is equally unresolved. The latter question, which is a central topic in the reaction mechanism, includes the nature of the active adsorbed oxygen species, e.g., a molecular species or an atomic one, and that of the active site for oxygen activation and its location on the catalyst, e.g., on the Au particle, on the TiO_2 support surface, or at the perimeter of the interface between these two.

In the present study, the latter questions were investigated by TAP reactor ('temporal analysis of products') measurements, focusing on two questions: (i) whether measurable amounts of oxygen species reactive for the CO oxidation can be stored on the surface of a Au/TiO_2 catalyst at a typical reaction temperature of 80 °C and, if so, (ii) whether the oxygen species reversibly stored and removed on the surface are also the active oxygen species in the dominant reaction pathway for CO oxidation. Further mechanistic information, in particular on the nature of the active site, is expected from possible correlations between the catalytic activity, oxygen storage capacity, and Au particle size at constant Au loading.

With the TAP reactor method introduced by Gleaves et al. [17], it is possible to detect and quantify even small amounts of reactants which are reversibly or irreversibly adsorbed on dispersed catalysts under ultra-high vacuum (UHV) conditions. This method has been applied for numerous studies on the mechanism and dynamics of adsorption and catalytic reaction processes on catalyst surfaces (see, e.g., Refs. [18] and [19,20] and the following papers in that Special Issue). In the recent years, this method was also applied for studies of the CO oxidation reaction on Au/TiO_2 catalysts

* Corresponding author. Fax: +49 731 50 25452.
E-mail address: juergen.behm@uni-ulm.de (R.J. Behm).
[1] Present address: Johnson Matthey Catalysts (Germany), Bahnhofstr. 43, D-96257 Redwitz, Germany.
[2] Present address: Dept. of Chemical Engineering and Center for Catalytic Science and Technology (CCST), University of Delaware, Newark, DE 19716-3110, USA.

0021-9517/$ - see front matter © 2009 Elsevier Inc. All rights reserved.
doi:10.1016/j.jcat.2009.03.013

[21–25]. The authors of these studies concluded that (i) O_2 and CO adsorb reversibly at room temperature and above (irreversible molecular oxygen adsorption at high pulse intensities), while CO_2 was proposed to adsorb irreversibly as carbonate-like species, (ii) CO does not react with lattice oxygen, (iii) the lifetime of adsorbed CO is long enough that it can react with a subsequent O_2 probe pulse (time delay between 50 and 10.000 ms), and (iv) the reaction involves molecular oxygen as reacting species. Recently, we used TAP reactor measurements to detect and quantify the amount of active oxygen species, active for CO oxidation, on the surface of a Au/CeO_2 catalyst [26]. These measurements not only revealed that CO clearly reacts with oxygen present on the catalyst, in the absence of a simultaneous O_2 pulse, but also revealed that the reactively removed oxygen can be reversibly 'refilled' by O_2 pulses and that oxygen removal leads to an activation of the catalyst for CO oxidation during simultaneous CO and O_2 pulses [26]. Obviously, these results, which contrast those reported by Olea et al., were obtained on a catalyst (Au/CeO_2) that was different from that studied by Olea et al. (Au/TiO_2), and CeO_2 is known for its facile participation of lattice oxygen in catalytic oxidation reactions [27–29] (in a Mars-van Krevelen type reaction mechanism [30]). Nevertheless, it seems to be highly interesting to exploit the high stability and reproducibility of our home-built TAP reactor [31] to perform similar studies also on a Au/TiO_2 catalyst, and in addition test for Au particle size effects on the above-mentioned properties.

For the present study, we prepared Au/TiO_2 catalysts with constant Au loading, but varied the Au particle size by using different temperatures in the subsequent conditioning step (calcination between 400 and 700 °C). The morphology, structure, and chemical composition of the resulting catalysts were characterized by transmission electron microscopy (TEM), X-ray photoelectron spectroscopy (XPS), X-ray diffraction (XRD), and low-temperature nitrogen adsorption. The amount of active oxygen species on the catalysts was investigated by multi-pulse and single-pulse TAP reactor measurements; the CO oxidation activities of the catalysts were evaluated both under close to ultra-high vacuum (UHV) conditions (TAP reactor) and under atmospheric pressure (fixed bed reactor). The resulting correlations between reversibly removed/stored oxygen, CO oxidation activities, and Au particle size or Au surface area are discussed in terms of the different mechanistic concepts, with special emphasis on the nature of the active oxygen species and its adsorption site.

2. Experimental

The Au/TiO_2 catalyst was prepared via a deposition-precipitation method using commercial, non-porous TiO_2 (P25, Degussa) as support material (surface area 56 $m^2\ g_{cat}^{-}1$) [32,33]. The Au loading was 3.4 wt.% Au for all samples. The synthesis procedure, the activity of these catalysts for CO oxidation at atmospheric pressure, and their deactivation behavior were described in detail previously [32,33]. To obtain catalysts with different Au particle sizes, the catalyst was pre-treated *ex situ* in air by calcination at temperatures of 400, 500, 600, and 700 °C for 2 h, the different procedures are denoted as C400, C500, C600, and C700, respectively. For comparison, in previous reaction measurements catalyst pre-treatment involved 30 min calcination at 400 °C (10% O_2, rest N_2), and calcination was performed *in situ* in the reactor directly before the reaction measurement [34,35]. To exclude subsequent modifications of the catalysts with time [36], the samples were stored in the dark in a refrigerator. The resulting Au/TiO_2 catalysts were characterized by (i) transmission electron microscopy (TEM), (ii) X-ray photoelectron spectroscopy (XPS), (iii) X-ray diffraction (XRD), and (iv) low-temperature nitrogen adsorption (BET) to obtain information on (i) the size and (ii) the oxidation state of the gold nanoparticles, (iii) the particle size and crystal phase of the titania support, and (iv) the surface area of the catalysts.

Catalytic activities were measured at atmospheric pressure and at 80 °C in a quartz tube microreactor (i.d. 4 mm), heated by a ceramic tube furnace with a gas flow rate of 60 Nml min^{-1} (1 kPa CO, 1 kPa O_2, and balance N_2). High-purity gases from Westphalen (CO 4.7, N_2 6.0, and O_2 5.0) were mixed via mass flow controllers (Hastings HFC-202). The effluent gases were analyzed by on-line gas chromatography using H_2 as a carrier gas (DANI, GC 86.10). Further details on the reactor set-up, the gas-mixing unit, and the data evaluation are given elsewhere [37]. The catalysts were diluted with α-Al_2O_3, which is not active for the reaction under the present reaction conditions, to obtain differential reaction conditions (CO conversion below 10% for all kinetic measurements) and hence to avoid mass and heat transport limitations as well as to guarantee isothermal reaction conditions.

The pulse experiments were carried out in a home-built TAP reactor [31], which is largely based on the TAP-2 approach of Gleaves et al. [38]. In short, piezo-electric pulse valves were used to generate gas pulses of typically 1×10^{16} molecules per pulse. The pulses were directed into a quartz tube microreactor with a length of 90 mm, an outer diameter of 6 mm, and an inner diameter of 4 mm. The reactor was heated by a ceramic tube furnace (Watlow GmbH), which can reach temperatures up to 900 °C. Thirty milligrams of the pure pre-treated catalyst were fixed in the central part of the reactor tube by stainless steel sieves (Haver& Boecker OHG), which are catalytically inactive under these conditions. This results in a catalyst bed length of about 6 mm. After passing through the catalyst bed and a differentially pumped gate valve, the gases propagated into the analysis chamber where they were analyzed by a quadrupole mass spectrometer (Pfeiffer Vacuum, QMG 700). In the analysis chamber, a base pressure of $<2 \times 10^{-9}$ mbar was generated by two turbomolecular pumps (Pfeiffer Vacuum, TPU 2101P and TMU 1001P) and was measured by a full range pressure gauge (Pfeiffer Vacuum, PKR251). The home-developed differentially pumped gate valve can (i) connect the end of the reactor directly to the analysis chamber, (ii) close the reactor and analysis chamber for sample exchange, or (iii) close only the analysis chamber and open the reactor to be pumped off or being operated under continuous flow conditions at atmospheric pressure [31]. Typically, the TAP measurements were performed at 80 °C, either in multi-pulse experiments for the determination of the OSC, pulsing subsequently only 80% O_2/20% Ar or 80% CO/20% Ar mixtures, or with simultaneous pulses of the O_2/Ar and CO/Ar mixtures to test the catalyst activity for CO oxidation. In both cases, the Ar component in the gas mixture was used as an internal standard for the data evaluation. With multi-pulse experiments, we quantified the amount of removable oxygen which can be reversibly stored and reactively removed on the catalyst surface. For this purpose, the fully oxidized catalyst was first reduced using a sequence of 100 pulses of CO/Ar and subsequently re-oxidized using a sequence of 100 pulses of O_2/Ar with separations of 30 s (CO) and 5 s (O_2) between the individual pulses, respectively. (The different waiting times between the pulses were chosen because of the different decay times of the reactant/product responses in the respective pulse sequences.) This way, two alternating sequences of CO/Ar and O_2/Ar pulses result in one complete reduction/re-oxidation cycle. This procedure was repeated at least five times on all samples. Prior to a change of the gas mixture, it was ensured that there was no more CO or O_2 consumption, i.e., that the catalyst was completely saturated with or replenished of removable oxygen. Because of the rather low temperature and the duration of the pulse sequences (8 min for the O_2 pulse sequence and 50 min for CO), oxygen storage can be assumed to be an essentially pure surface reaction. CO conversion on the Au/TiO_2 catalysts with different Au particle sizes under vacuum condi-

tions was measured by simultaneous pulses with a time delay of 30 s between subsequent pairs of pulses.

XPS measurements were performed on a PHI 5800 ESCA system (Physical Electronics), using monochromatized Al–K_α radiation. TEM images were acquired in the Central Facility for Electron Microscopy, employing a Philips CM 20 instrument (200 keV). XRD and BET measurements were carried out in the Institute of Nano and Micromaterials (Ulm University, Siemens diffractometer D5000) and in the Institute of Inorganic Chemistry (Ulm University, Autosorp MP1, Quantachrome), respectively.

3. Results and discussion

3.1. Catalyst characterization

The morphology of the Au/TiO_2 catalysts after the different pre-treatment procedures is well resolved in the TEM images shown in Fig. 1. They clearly demonstrate the increase of the Au particle size with increasing pre-treatment temperature. For the Au particle size determination, we averaged over several hundred particles for every catalyst (>500 particles for C400 → >300 particles for C700). The mean diameter of the Au particles increased in the following order: 3.5 ± 0.9, 4.8 ± 1.0, 6.7 ± 1.5, and 11.6 ± 3.1 nm for C400, C500, C600, and C700, respectively (see also Table 1). Moreover, the distribution of the Au particle size became wider with increasing pre-treatment temperature, which is illustrated in the particle size distributions shown in Fig. 2. The Au surface area was calculated assuming hemispherical particles, which resulted in values of 3.0, 2.2, 1.6, and 0.9 $m^2\ g_{cat}^{-1}$, respectively [39].

XPS measurements of the catalysts (*ex situ* after conditioning) showed that Au mainly exists in its metallic state (Au^0) (Au(4f) binding energy ~84.0 ± 0.1 eV) after pre-treatment and that the amount of Au^{3+} (Au(4f) binding energy ~85.9 ± 0.1 eV) is about the same (~5%) for all samples (spectra not shown).

In addition to the growth in Au particle size, the TEM images also revealed a significant growth of the TiO_2 support particles, at least for the C700 sample. Therefore, additional XRD measurements were performed on the C400–C700 samples, where diffraction spots indicative of rutile and anatase phases could be identified. (P25 consists of a mixture of anatase and rutile phases.)

Table 1
Physical properties, catalyst activity, and oxygen storage capacity (OSC) of the Au/TiO_2 catalyst after different pre-treatment procedures as indicated.

	C400[a]	C500[a]	C600[a]	C700[a]
Au diameter (nm)[b]	3.5 ± 0.9	4.8 ± 1.0	6.7 ± 1.5	11.6 ± 3.1
Au surface area ($m^2\ g_{cat}^{-1}$)[c]	3.0	2.2	1.6	0.9
Length of the perimeter of the Au-TiO_2 interface ($m^2\ g_{cat}^{-1}$)	1.6×10^9	8.6×10^8	4.5×10^8	1.5×10^8
Particle size rutile (nm)[d]	31	34	41	73
Particle size anatase (nm)[d]	21	21	23	22
Catalyst surface area ($m^2\ g_{cat}^{-1}$)[e]	46	46	41	28
Initial TOF (s^{-1})	0.35	0.28	0.21	0.08
TAP: CO conversion (%) in steady-state	83	63	46	21
TAP: OSC (molecules $O_2\ g_{cat}^{-1}$)	2.2×10^{18}	1.4×10^{18}	9.6×10^{17}	5.3×10^{17}

[a] Au loading 3.4 wt.%.
[b] Determined by TEM.
[c] Assuming half spherical particles.
[d] Determined by XRD.
[e] Determined by low-temperature nitrogen adsorption (BET).

Evaluation of the diffractograms via the Scherrer equation showed that the domain sizes of the rutile phase increase with increasing pre-treatment temperature, resulting in mean widths of 31 nm (C400), 34 nm (C500), 41 nm (C600), and 73 nm (C700), respectively. On the other hand, the domain size of the anatase phase was almost constant for all samples (21, 21, 23, and 22 nm). At the same time, the relative amount of rutile phase increased with increasing pre-treatment temperature, indicated by the increasing rutile and a decreasing anatase signal intensity with increasing annealing temperature. This can be explained by a phase transition of TiO_2 from anatase to rutile at higher temperatures and a parallel growth of the rutile particles due to sintering, which is especially prominent at the highest pre-treatment temperature (C700).

Measurements of the surface area of the samples by nitrogen adsorption (BET) performed after the different pre-treatment procedures confirmed this trend, showing a decrease in the surface area with increasing temperature from 46 $m^2\ g_{cat}^{-1}$ for the C400 and C500 samples to 28 $m^2\ g_{cat}^{-1}$ for the C700 sample. The resulting structural data are summarized in Table 1.

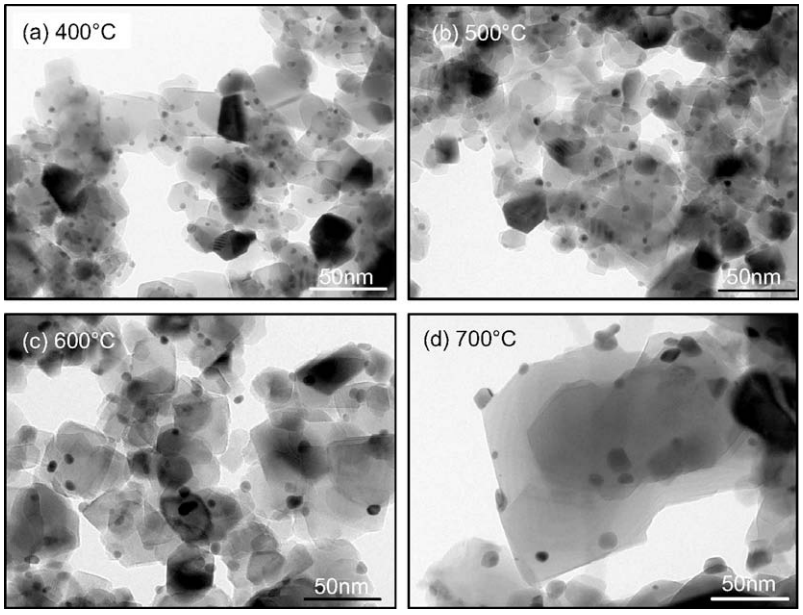

Fig. 1. Representative TEM images of the Au/TiO_2 catalyst after calcination in air for 2 h at (a) 400 °C, (b) 500 °C, (c) 600 °C, and (d) 700 °C, respectively.

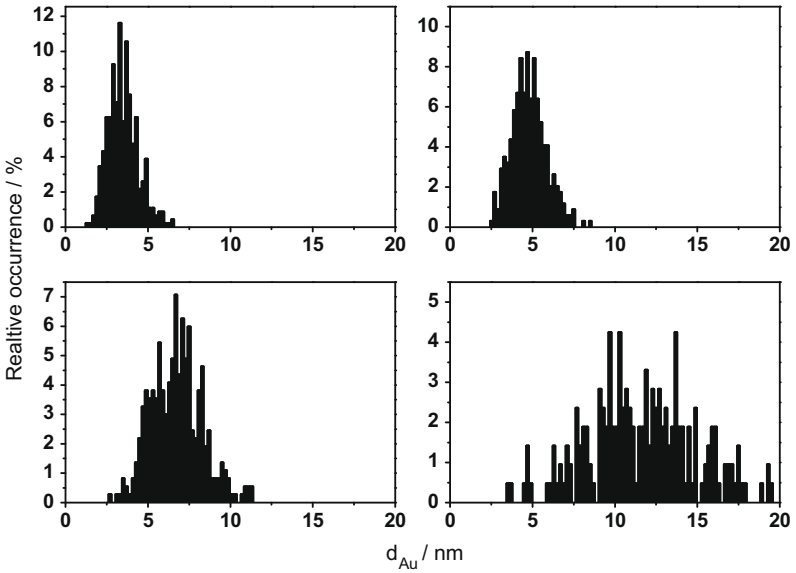

Fig. 2. Particle size distributions of the Au/TiO_2 catalysts after calcination in air for 2 h at (a) 400 °C, (b) 500 °C, (c) 600 °C, and (d) 700 °C, respectively.

3.2. Kinetic measurements

The activities of the differently pre-treated Au/TiO_2 catalysts for CO oxidation and their development with time were determined in a standard reaction mixture (1 kPa CO, 1 kPa O_2, and rest N_2) at a reaction temperature of 80 °C. The results of the activity measurements are presented in Fig. 3. To correct for effects induced by Au particle growth, the reaction rates were described in terms of turnover frequencies (TOF, molecules CO_2 per Au surface atom per second), which are normalized to the Au surface atoms of the respective catalysts. (For Au surface atoms see Table 1, absolute rates can be calculated by using the relations 1 $s^{-1} = x$ mol CO_2 g_{Au}^{-1} s^{-1}, with $x = 5.2 \times 10^{-4}$ (C400), $x = 3.1 \times 10^{-4}$ (C500), $x = 1.7 \times 10^{-4}$ (C600), and $x = 3.4 \times 10^{-5}$ (C700).) The C400 data showed a typical reaction behavior of these catalysts, with an initial decay of the activity by 20–30%, while the activity was lower than that in the previous measurements [35,40]. The latter may be related to the slightly different calcination procedure (*ex situ* calcination including subsequent exposure of the catalyst to air) and the longer calcination time (2 h vs. 30 min).

As expected, the initial activity of the samples decreased with increasing pre-treatment temperature and increasing Au particle size. The corresponding TOF numbers are 0.35, 0.28, 0.21, and 0.08 s^{-1} respectively (see also Table 1). Similar Au particle size effects, using Au size-normalized TOF numbers, were reported previously by a number of other groups [11,41–45] and were explained by different effects, ranging from quantum size effects [44] via a size-related decrease in the number of under-coordinated Au sites [10,11,46] or under-coordinated Au sites at the perimeter of the interface between Au nanoparticle and TiO_2 support [8,11,13–15] to cooperative effects between metallic and cationic Au species [6–8]. In X-ray absorption measurements, Miller et al. found that only Au atoms in particles smaller than 3 nm can be partly oxidized in air and suggested these to be active for CO oxidation [47].

We need to consider, however, that in addition to the Au particle growth the size of the rutile particles also increased and that anatase was transformed to rutile. The crystalline structure of the TiO_2 support may also affect the catalytic behavior of Au/TiO_2. For instance, Haruta et al. reported that the reaction pathway on their Au/TiO_2 catalyst in the conversion of propylene in a gas stream containing hydrogen and oxygen differed for rutile- and anatase-supported Au/TiO_2 [48]. On the other hand, a higher activity of Au/TiO_2 catalysts with rutile supports than that of those supported on anatase can hardly be the dominant reason for the observed decrease in the activity of C400–C700 catalysts, since the transition from anatase to rutile phase and the parallel growth of the rutile domains became significant only for the C700 sample, while the activity had already decreased for the C500 sample compared to the C400 sample. The C500 and C400 samples are essentially identical in TiO_2 phase composition and particle size, and differ only in the Au particle size. Therefore, we assume that the decrease in the catalyst activity (TOF numbers) with calcination temperature is mainly related to the increase of the Au particle size. Most simply, this can be explained by a decrease in the absolute number of Au surface atoms, of under-coordinated Au atoms, or of Au atoms at that perimeter sites of the interface between the Au particles and the support, though other effects cannot be excluded as the physical origin.

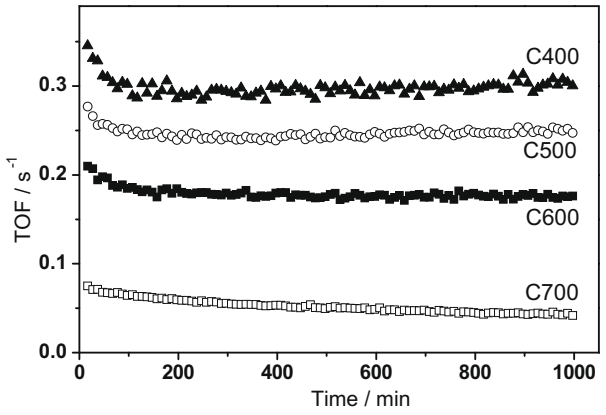

Fig. 3. Turn-over frequencies (TOF) during CO oxidation on differently pre-treated Au/TiO_2 catalysts after calcination in air for 2 h at 400 °C (▲), 500 °C (○), 600 °C (■), and 700 °C (□) (reaction temperature 80 °C, 1 kPa CO, 1 kPa O_2, and balance N_2).

3.3. TAP experiments

3.3.1. Multi-pulse TAP experiments

Multi-pulse TAP experiments, exposing the pre-reduced catalyst to a sequence of O_2 pulses or the pre-oxidized catalyst to a

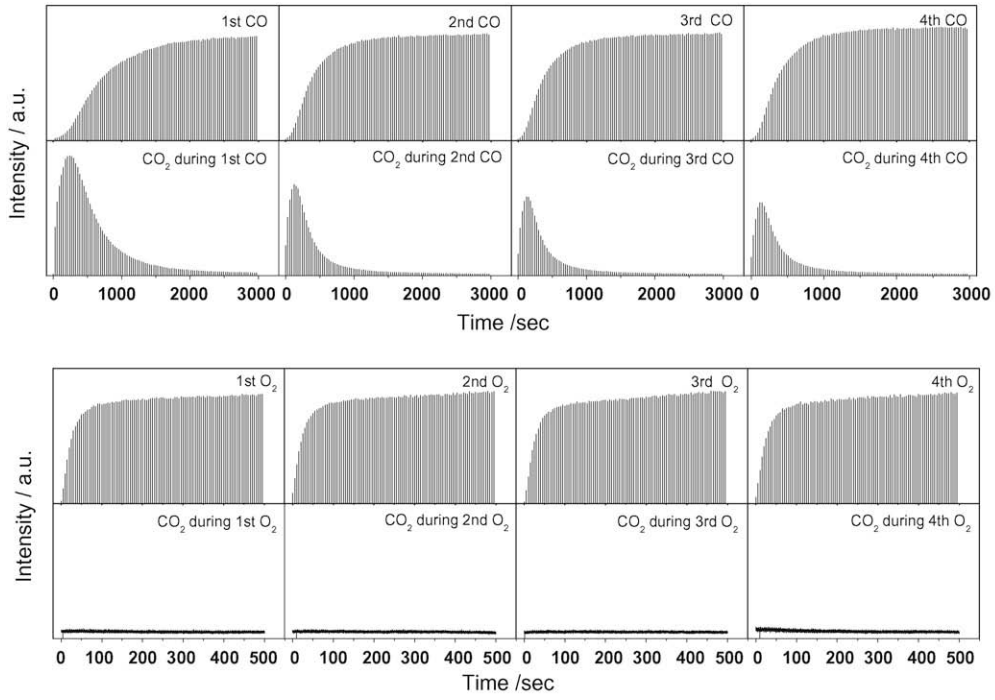

Fig. 4. Pulse responses during a multi-pulse experiment performed at 80 °C over the Au/TiO_2 catalyst after calcination in air for 2 h at 400 °C (C400).

sequence of CO pulses, were carried out on all of the differently pre-treated catalysts. In the first sequence, the *ex situ*-calcined catalyst was exposed to O_2 (no adsorption observed) and then to alternating sequences of CO pulses and O_2 pulses. Representative pulse responses for the multi-pulse experiments on the C400 and C700 samples are presented in Figs. 4 and 5, respectively.

The shapes of the CO and O_2 signals closely resemble that of the Ar signals, with no significant broadening. Accordingly, the interaction between the species detected in the pulse response and the Au/TiO_2 catalyst is rather weak. On the other hand, the CO_2 signals are significantly broader, and their trailing edge reaches up to the next pulse after 10 s, pointing to a stronger interaction with the catalyst (slower desorption/re-adsorption). This is illustrated and discussed in more detail in the following section, together with Fig. 9.

The pulse sequences clearly show that after passing through the catalyst bed, the first CO pulses have a significantly lower intensity than the later ones. Parallel to the loss of CO, the formation of CO_2

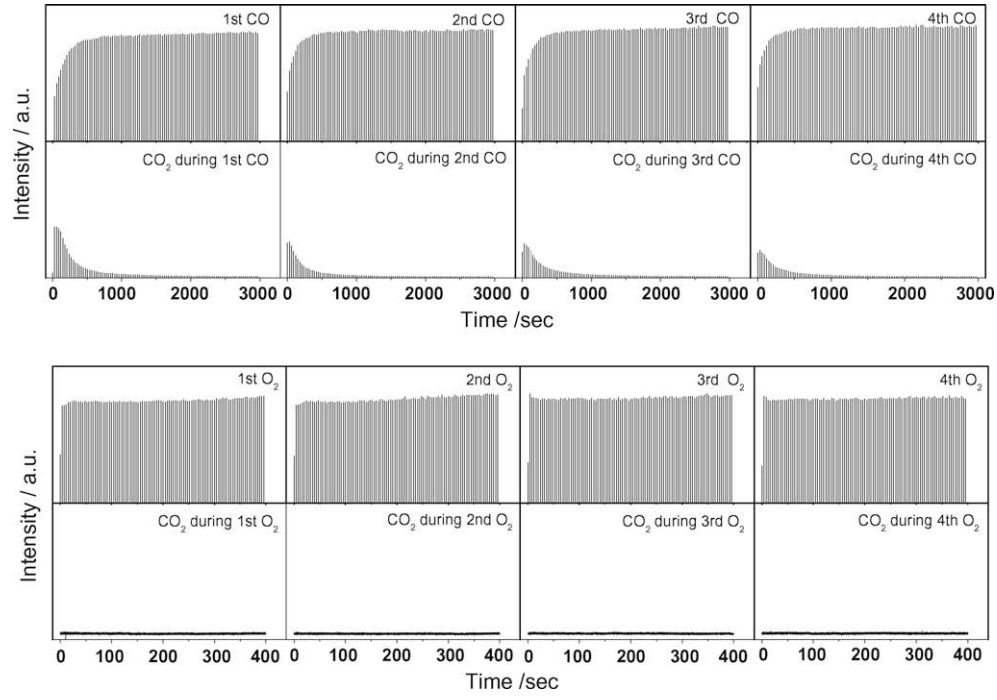

Fig. 5. Pulse responses during a multi-pulse experiment performed at 80 °C over the Au/TiO_2 catalyst after calcination in air for 2 h at 700 °C (C700).

was observed during the CO pulses, in spite of the absence of gas phase O_2, indicating that CO reacts with oxygen species already present on the catalyst surface. For all CO pulse sequences, the total amount of CO missing was highest at the beginning of the CO pulse sequence, where essentially no CO was transmitted (100% conversion), and it decreased with increasing pulse number until it decayed to zero after about 50 pulses for the C400 sample. In the first sequence, the amounts of CO consumed and of CO_2 produced were higher than those consumed and produced in the second and following ones, where they remained on the same level. In contrast to the CO consumption, however, the CO_2 formation first increased during the first ~10 pulses and then decreased again steadily, following an approximately exponential decay. Finally, it decayed to the detection limit after ~60 pulses. After typically 100 CO pulses, the catalyst was exposed to a sequence of 100 O_2 pulses (see lower trace in the bottom panel of Fig. 4). Also in this sequence, part of the oxygen was consumed initially, until after ~40 pulses oxygen consumption was no longer measurable. In contrast to CO pulsing, the amount of oxygen consumed was the same in all O_2 pulse sequences. Moreover, we did not observe any CO_2 formation during the O_2 pulses. Thus, there is no reactive CO adsorbed on the catalyst any more after the time delay of about 5 s between the last CO pulse and the first O_2 pulse. Instead, the 'consumed' oxygen is stored on the catalyst.

The C700 sample (Fig. 5), and also the samples calcined at intermediate temperatures, exhibited an adsorption/reaction behavior that was qualitatively similar to that observed for the C400 sample. The total amount of O_2 and CO consumed at the beginning of each sequence, however, was less than that consumed after C400 pretreatment (see Table 1). Furthermore, a significantly lower number of CO pulses were required to remove the reactive surface oxygen on the C700 sample than that required for the C400 sample, about ~25 pulses compared to ~50 pulses, and a similar trend was also observed for oxygen replenishment (~20 vs. ~40 pulses, respectively), pointing to a lower OSC on the C700 sample than on the C400 catalyst.

The total amount of the removable oxygen is rather small, depending on the catalyst it is between 0.4% (C700) and 1.0% (C400) of the entire surface oxygen content. (The surface oxygen content was calculated by using the surface area of the catalyst given in Table 1 and a density of surface oxygen atoms of 1.0×10^{15} atoms cm^{-2}.) Furthermore, the OSC decreases with increasing pre-treatment temperature, and hence with increasing gold particle size. Relating the OSC to the number of Au surface atoms yields a value of about 0.1 removable oxygen atoms per Au surface atom (C400: 0.13, C500: 0.11, C600: 011, and C700: 0.10.). In order to compare with previous ideas on the active site, we plotted the amount of reversibly removable oxygen present on the different catalysts in Fig. 6 against the calculated total length of the accessible perimeter of the interface between Au nanoparticles and TiO_2 support, assuming hemispherical particle shapes and the particle size distributions shown in Fig. 2. The data show an approximately linear correlation between the OSC and the Au perimeter length, with local oxygen coverages of 0.89 (C400), 1.04 (C500), 1.36 (C600), and 2.21 (C700), where the coverage is again defined as ratio between oxygen atoms and Au perimeter atoms. Except for the C700 value, this corresponds to approximate saturation of the Au perimeter sites. Based on previous calculations, oxygen is likely to be adsorbed in a molecular state [15], which leads to molecular coverages between 0.45 (C400) and 1.1 (C700). Although the good agreement between the availability of perimeter sites and the OSC is no definite proof for the perimeter sites as active sites for oxygen adsorption, the good correlation between OSC and Au-TiO_2 interface perimeter is definitely a strong support for this assignment. Furthermore, considering the above numbers, essentially all the perimeter sites need to be active for oxygen storage/reactive oxygen removal. Further structural requirements such as 'step sites at the perimeter' are hardly compatible with the measured OSC. The physical origin of the increasing OSC per Au perimeter atom with increasing calcination temperature and Au particle size, in particular for the C700 species, is not clear yet. (Note that deviations from the assumed hemispherical shape may also affect these values.) Other possibilities for active oxygen storage, such as the incorporation of (atomic) oxygen in oxygen surface vacancies of the support or the stabilization of molecularly adsorbed oxygen on these vacancies, appear unlikely, because in the first case it could hardly be rationalized how oxygen could be removed in the subsequent CO sequence from the resulting perfect TiO_2 surface, and in the second case reversible removal and replenishment should also be possible on pure TiO_2, in the absence of Au nanoparticles. Test measurements clearly demonstrated that this is not the case, the presence of Au nanoparticles is mandatory for reversible oxygen storage on the catalyst under the present reaction conditions. A more detailed discussion of the nature of the active oxygen species will be given at the end of Section 3.3.2.

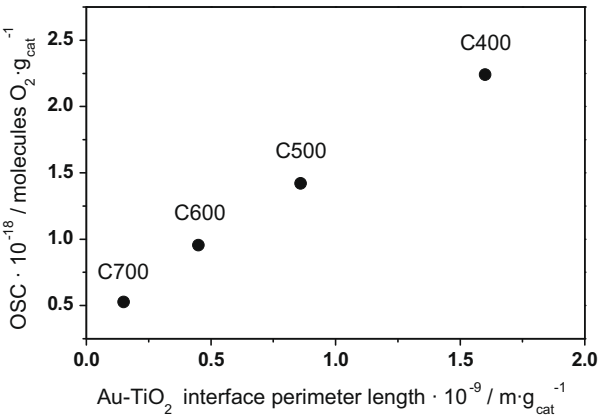

Fig. 6. Oxygen storage capacity of the Au/TiO_2 catalysts in multi-pulse experiments at 80 °C after calcination in air for 2 h at various temperatures plotted against the length of the Au-TiO_2 interface perimeter.

Also in this case, possible effects of the TiO_2 phase of the catalyst cannot be ruled out *per se*. Similar to the catalyst activity, however, the OSC changes to a significant amount for the C500 sample compared to the C400 sample, and continues to change for higher annealing temperatures, in contrast to the changes of the crystalline phase, which are appreciable only for the highest calcination temperature (C700). Therefore, we consider OSC modifications related to the change in substrate phase only as a secondary effect.

Fig. 7 shows the consumptions of CO and O_2 on the C400 sample in several sequences of the multi-pulse experiment at 80 °C. Except for the first sequence, constant and stoichiometric amounts of CO and O_2 were consumed, i.e., the amount of CO consumption was twice the amount of O_2 consumed, indicating a completely reversible oxidation-reduction behavior of the surface after the first reduction sequence. Only in the first sequence, the amount of consumed CO was significantly higher (8.6×10^{18} molecules g_{cat}^{-1}), by about a factor of two, than that consumed in the following sequences (4.3×10^{18} molecules g_{cat}^{-1}). At the same time, the amount of CO_2 detected was also higher than that detected in the following sequences, but this difference was somewhat smaller than that observed for reactive CO removal, with 7.4×10^{18} molecules g_{cat}^{-1} during the first sequence and $\sim 4.3 \times 10^{18}$ molecules g_{cat}^{-1} in the subsequent ones. The more pronounced CO_2 formation in the first sequence points to a higher amount of reversibly removable 'active' oxygen after calcination as compared to re-oxidation via O_2 pulsing. The higher amount of missing CO as compared to CO_2 formation in the first cycle, in contrast, points to a process for CO con-

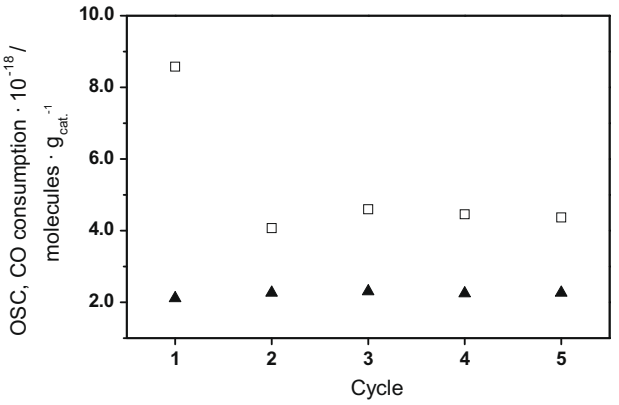

Fig. 7. Total amount of CO (□) and O_2 (▲) consumed during the multi-pulse experiment at 80 °C on the Au/TiO_2 catalyst after calcination in air for 2 h at 400 °C (C400).

sumption which involves stable CO (or CO_2) deposition. Previous *in situ* IR studies detected the rapid buildup of surface carbonates during CO oxidation on Au/TiO_2 catalysts [34,35,49–51]. Accordingly, the consumption of excess CO, without CO_2 formation, is attributed to the formation of surface carbonates, which are adsorbed irreversibly on the catalyst surface, as the most plausible reaction pathway.

The total amount of CO storage via carbonate formation, which was around 1.5×10^{18} molecules g_{cat}^{-1} for the C400 sample, was found to vary measurably, which may be related to details in the pre-treatment procedure and hence to different carbonate coverages (residua after calcination) at the beginning of the experiment. For the C500–C700 treated samples, carbonate formation was too little to allow quantitative statements. Carbonate decomposition upon exposure to O_2 during O_2 pulses, as it was observed upon calcination of Au/CeO_2 catalysts [52], was not detected and must be, if occurring at all, below the detection limits.

Our data differ distinctly from previous findings by Olea et al., which were obtained in TAP experiments using partly hydroxylated Au/TiO_2 catalysts ($Au/Ti(OH)_4^*$) [21,22]. By performing pump-probe CO oxidation experiments with O_2 as a pump molecule and CO as a probe molecule, these authors found that the CO conversion and CO_2 formation decrease with increasing time delay between the O_2 and CO pulses and concluded that lattice oxygen does not contribute to the CO oxidation reaction. Instead, oxygen adsorbed from the gas phase was proposed to be necessary for the formation of CO_2. Although our multi-pulse experiments differ from the above pump-probe measurements in that the time between the (last) O_2 pulse and the (first) CO pulse was not varied, they clearly indicate that surface oxygen of the catalyst can participate in the reaction in well-defined amounts. In fact, in additional experiments not described explicitly it turned out that the 'active' oxygen was stable over hours. On the other hand, from the results of CO pump/O_2 probe experiments the above authors also derived that CO remains sufficiently long adsorbed on the catalyst surface to react with a subsequent O_2 pulse after up to 10 s, which is in clear contrast to our observation of no CO_2 formation during the O_2 pulse. The different results may be due to a different surface chemistry of the Au/TiO_2 catalysts used in the two studies. Another and to our belief more likely possibility to explain the claimed stronger adsorption of CO may be differences in the TAP experiments, including the catalyst bed packing, and hence in the CO diffusion time. The initial removal or replenishment of oxygen is possible only in measurements based on the time-resolved analysis of single pulses, whereas in the commonly used pulse shape analysis, using an average of several hundred pulses for improving the signal-to-noise ratio, the initial differences in the pulse intensities would be lost. Furthermore, in the above study, the CO pulses extended over significantly more than 10 s, i.e, even after 10 s there was still gaseous CO in the catalyst bed, and it was not necessary to invoke 'stronger' CO adsorption. In our experiments, in contrast, the CO pulse had decayed to intensities below the detection limit after ~3 s significantly before the next O_2 pulse.

3.3.2. Simultaneous-pulse TAP experiments

In a second series of experiments, the development of the CO oxidation activity (CO_2 formation) was followed during sequences of mixed CO/O_2/Ar pulse (CO: O_2 = 1.1:1) at a reaction temperature of 80 °C together with the consumption of CO and O_2, starting with the calcined catalyst sample. These data allow us to determine (i) the balance between CO and O_2 consumption on the one hand and CO_2 formation on the other hand, and (ii) the balance between CO consumption and O_2 consumption as a function of time during the reaction. In Fig. 8, the amounts of the reactants consumed (CO and O_2) and CO_2 formed during these pulses are plotted for the C400 sample as a function of the pulse number.

Both O_2 consumption and CO_2 formation started at rather low values and increased with time. The consumption and conversion of CO, in contrast, were highest at the beginning, and then decreased with time. (Note that the first lower CO value is an experimental artifact, which occurs reproducibly and should be disregarded [26].) After an initial period of about 45 pulses, the amount of CO_2 produced and the consumption of CO and O_2, respectively, reached a constant value. From there on, stoichiometric amounts of the two reactants were consumed, and a corresponding amount of CO_2 was formed, hence the consumed CO and O_2 are quantitatively transformed into CO_2. These results lead to two conclusions: First, they clearly indicate that the reaction of CO with oxygen from the catalyst surface occurs even in the presence of gas phase O_2. This is more far reaching than our conclusion from the multi-pulse experiments, where we showed that reaction with oxygen on the catalyst surface is possible in the absence of gaseous O_2. Second, the results demonstrate that at the beginning of the reaction sizable amounts of CO are reactively consumed without leaving the catalyst bed as CO_2, but remain adsorbed on the catalyst surface. As discussed in the preceding section, a simple storage of CO adsorbed on the catalyst surface can be excluded, and the loss of CO is attributed to the formation of stable adsorbed species, presumably surface carbonates (see also Section 3.3.1), in the very initial phase of the reaction. From the difference in the CO and CO_2 balance, the total amount of adsorbed carbonate species can be

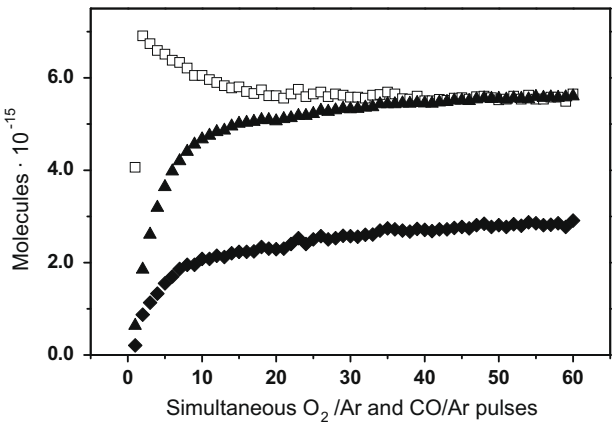

Fig. 8. CO uptake (□), O_2 uptake (◆), and CO_2 formation (▲) during simultaneous CO/Ar and O_2/Ar pulses at 80 °C on the Au/TiO_2 catalyst after calcination in air for 2 h at 400 °C (C400).

estimated to 4.2×10^{16} molecules (1.4×10^{18} molecules g_{cat}^{-1}) on the C400 pre-treated catalyst equivalent to a density of 3.1×10^{12} molecules cm^{-2}. For the other catalysts pre-treated at higher temperatures, the corresponding numbers are 3.1×10^{16} molecules (1.0×10^{18} molecules g_{cat}^{-1}) or 2.3×10^{12} molecules cm^{-2} (C500), 2.7×10^{16} molecules (9.0×10^{17} molecules g_{cat}^{-1}) or 2.2×10^{12} molecules cm^{-2} (C600), and 2.5×10^{16} molecules (8.2×10^{17} molecules g_{cat}^{-1}) or 2.9×10^{12} molecules cm^{-2} (C700). Quantitative comparison of the above numbers leads to the conclusion that within the limits of their precision (see Section 3.3.1) the resulting carbonate coverages (per catalyst surface area) are similar on all samples. Pulse experiments over pure TiO_2using labeled $C^{18}O_2$ (not shown here) clearly demonstrated that the Au-free surface also strongly interacts with CO_2, up to the facile exchange of oxygen. Most probably, this occurs via the formation and (CO_2 induced) decomposition of surface carbonates, supporting our above interpretation that the additional consumption of CO is due to CO_2 formation and its subsequent reaction to surface carbonate species.

From the steady increase in CO_2 formation with increasing pulse number, it is clear that the Au/TiO_2 catalysts are activated in the initial phase of the CO oxidation reaction. The activation, however, is mainly due to the decreasing consumption of CO and/or CO_2 for surface carbonate formation rather than due to a lower CO uptake at the onset of the reaction in the first pulses. The latter in fact decreases during the initial stage of the reaction (see above). The consumption of CO/CO_2 for surface carbonate formation occurs in parallel with the initial removal of surface oxygen from the catalyst, i.e., it is likely that part of the surface oxygen is used to react CO to CO_2, which is then transformed to a surface carbonate.

Fig. 9 shows the TAP pulse responses of the CO, O_2, and CO_2 signals and, for comparison, of the Ar signal, after reaching a constant value on the C400 catalyst (catalyst temperature 80 °C). For better comparison, these signals are normalized to the same height. As noticed for the multi-pulse experiments before, the O_2 and CO pulse shapes are similar to the Ar pulse shape, with a similar broadening due to diffusion through the catalyst bed, which points to weakly adsorbed species with negligible contributions from re-adsorption/desorption. The CO_2 pulse shape, in contrast, shows a much longer tailing, which we attribute to contributions from desorption and re-adsorption of CO_2 and hence to a stronger interaction of CO_2 with the catalyst. Based on previous DRIFTS measurements, the decomposition of stable surface species such as formates or carbonates is too slow at 80 °C to be responsible for a pulse broadening on a second scale [53]. Our interpretation differs from that by Olea et al., who also observed a comparable broadening of the CO_2 pulse on their $Au/Ti(OH)_4^*$ catalyst and assigned this to the existence of a less reactive oxygen species and/or the slow decomposition of intermediate carbonates, which are built up on the catalyst surface during reaction [21]. Two independent pathways for the CO oxidation, a rapid direct oxidation of CO on the surface of the metallic Au particles and a slow reaction "involving the surface lattice oxygens of the support and the borderline of the gold particles", were suggested also by Boccuzzi et al. for CO oxidation on Au/ZnO and Au/TiO_2 catalysts [49]. Based on our present data, however, we consider such a mechanism for CO_2 pulse broadening as unlikely, since all CO, gaseous and adsorbed CO, left the catalyst bed after 3 s. Therefore, reaction of CO with a less reactive oxygen species cannot explain a CO_2 pulse broadening over 10–20 s, since there would be no CO available to react with.

The reaction behavior after higher pre-treatment temperatures (C500–C700) is qualitatively the same as described above for the C400 sample. On all samples, there is an increasing O_2 consumption and CO_2 formation parallel to the decreasing CO consumption directly after the calcination in air at the beginning of the activity

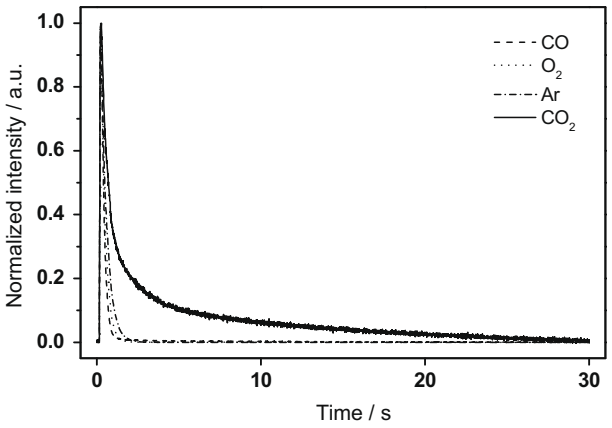

Fig. 9. Shapes of the height-normalized signals of Ar, O_2, CO, and CO_2 on the C400 Au/TiO_2 catalyst (calcination in air for 2 h at 400 °C) during the simultaneous pulse experiment at 80 °C in Fig. 8.

measurement. The data are accessible as Supplementary information.

Similar to the variation of the OSC with Au particle size, we also evaluated the variation of the CO conversion (CO consumption) during simultaneous CO and O_2 pulses under steady-state conditions at the end of the pulse sequence with the Au particle size. Fig. 10 shows a plot of the steady-state CO conversion vs. the Au-TiO_2 interface perimeter length. Also these data show an about linear correlation between CO oxidation activity and the Au-TiO_2 interface perimeter length, similar to the observations for the OSC in the multi-pulse experiments (previous section). The deviation of the C400 sample, however, is larger than that in the OSC shown in Fig. 6. We have to keep in mind, however, that the reactivity data represent the integrated conversion of CO over the catalyst bed, which for higher conversions as obtained on the samples pre-treated at lower temperatures (see Table 1) are not proportional to the rates for the given gas composition, but generally lower. Though a quantitative correction for this effect is not possible without extensive assumptions, this would shift the rates to increasingly higher values for decreasing calcination temperature [54].

The comparable variation of the OSC (Section 3.3.1) and of the CO oxidation activity with the Au-TiO_2 interface perimeter length indicates that the removable oxygen detected in the multi-pulse

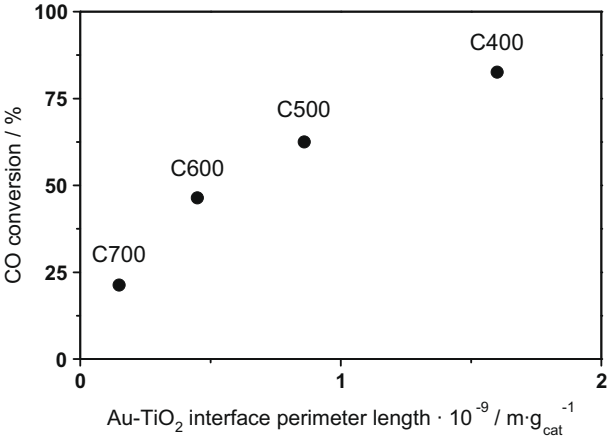

Fig. 10. Relative conversion of CO at 80 °C during simultaneous CO/Ar and O_2/Ar pulses over the Au/TiO_2 catalyst after calcination in air for 2 h at various temperatures plotted against the length of the Au-TiO_2 interface perimeter.

experiments acts also as active oxygen species in the CO oxidation reaction in the presence of gas phase O_2 and CO in the simultaneous pulse experiments. In that case, the stable adsorbed oxygen species can be considered as direct precursor for the CO oxidation reaction in the dominant pathway (see also [15]), while weakly adsorbed oxygen contributes at most in a minority reaction pathway under present reaction conditions. Furthermore, the about linear increase of the amount of stable adsorbed oxygen with the Au-TiO_2 interface perimeter length can be considered as strong evidence for an adsorption site at the perimeter of the interface between gold nanoparticles and the support. Finally, it should be noted that the trend in the CO conversion obtained under close to UHV conditions in the TAP measurements resembles that observed in the kinetic measurements under atmospheric pressure (Fig. 3), pointing to a similar reaction pathway and active oxygen species in both cases.

While it was possible to clearly identify the strongly adsorbed oxygen species as active reaction precursor, we cannot decide from these experiments on its specific nature, i.e., it is not possible to determine whether it is an atomic or a molecular species. In principle, this would be possible by reaction of $C^{16}O$ with isotope labeled $^{18}O_2$ (or vice versa). For reaction with a molecular O_2 species proceeding via a carbonate like transition state, one would expect a 2:1 ratio between $C^{16}O^{18}O$ and $C^{18}O_2$ [55]. Unfortunately, this experiment provides only limited information in the present case because of the rapid oxygen exchange between CO_2 and the TiO_2 support of the Au/TiO_2 catalyst [21]. In the case of a molecular oxygen species acting as a reaction precursor, the reaction with CO would lead to a 'remaining' O_{ad} intermediate on the surface, possibly on the Au nanoparticles. Since pre-adsorbed atomic oxygen on Au surfaces is well known to react at very low temperatures with CO [56], the remaining atomic O_{ad} species can be expected to rapidly react with another CO molecule without slowing down the reaction.

Likewise, we cannot distinguish between lattice oxygen (parallel to a local formation of Ti^{3+} at the surface) and adsorbed oxygen at the perimeter sites on the basis of the present experiments. A further possibility, reversible reduction and oxidation of cationic Au^{3+} species as active oxygen source, appears unlikely in our experiments, since it does not explain the systematic differences in the OSC on the differently pre-treated samples (the total amount of Au^{+3} species derived from XPS was about the same for all catalysts). Nevertheless, though unlikely, it cannot be fully ruled out if the systematic differences are induced by other effects.

Comparable results from TAP measurements were reported also by Daniells et al. for a Au/Fe_2O_3 catalyst [51] and by Widmann et al. for a Au/CeO_2 catalyst [26]: The former authors observed in simultaneous-pulse TAP experiments that adsorption of oxygen on the fresh Au/Fe_2O_3catalyst was not possible, and occurred only after CO oxidation. (Note that the catalyst was used without drying and/or pre-treatment.) They concluded that O_2 was stabilized by oxygen vacancies on the catalyst surfaces that had been or had to be created during a preceding CO oxidation reaction. Furthermore, they proposed that the adsorbing oxygen species was of molecular nature, most likely a superoxide O_2^- species. Definite proof of this assumption, however, was not presented [51]. Widmann et al. reported that during CO oxidation in simultaneous CO/Ar and O_2/Ar pulses both the consumption of CO and the formation of CO_2 increased steadily during an initial reaction phase. The calcined Au/CeO_2 catalyst underwent an initial activation period for CO oxidation, which was attributed to the creation of oxygen vacancies by reduction of the catalyst surface with CO. The amount of oxygen vacancies under steady-state conditions was determined to ~7% of the available surface oxygen. These vacancies were proposed to act as active sites for the adsorption and activation of molecular oxygen from the gas phase [26]. A similar initial reduction process also occurs for the present Au/TiO_2 catalysts, and the same is also true for the initial activation process, at least as judged by the initial increase in CO_2 formation. In contrast to the Au/CeO_2 catalyst, however, we do not observe an initial activation period for the CO oxidation reaction, when using the CO consumption as measure for the reaction. On the fully oxidized Au/CeO_2 catalyst also the amount of CO consumed per pulse increased with increasing number of pulses, while on Au/TiO_2 it decreased until reaching steady-state conditions. Hence, considering that also the surface carbonate species formed on the surface result from CO_2 which was formed on the catalyst and instantaneously reacted to this carbonate species, the fully oxidized Au/TiO_2 catalyst is highly active for CO oxidation, in contrast to Au/CeO_2. Partial surface reduction of the catalyst occurs on both catalysts during reaction in a 1.1:1 mixture of CO and O_2 at 80 °C. The amount of reversibly removable active oxygen, however, is much less for Au/TiO_2 (1% of the surface oxygen for C400) than for a similarly pre-treated Au/CeO_2 catalyst (16% of the surface oxygen) [26]. On Au/TiO_2, the initial surface reduction does not affect the activity for CO oxidation as judged by the consumption of CO, in contrast to the significant activation of Au/CeO_2 catalyst [26]. This also means that the composition of the reaction gas phase, which will determine the extent of surface reduction under steady-state conditions, will be less important for the CO oxidation activity for the Au/TiO_2 catalyst than for the Au/CeO_2 catalyst.

4. Summary and conclusions

We have investigated the CO oxidation reaction on Au/TiO_2 catalysts with different Au particle sizes by kinetic measurements under atmospheric pressure and by multi-pulse and single-pulse experiments in a TAP reactor at close to UHV conditions, focusing on the correlation between oxygen storage capacity and CO oxidation activity, and their relation with the Au particle size. Catalysts with different Au particle sizes were prepared by deposition/precipitation of Au on non-porous TiO_2 particles and subsequent calcination at different temperatures between 400 and 700 °C. TEM measurements showed that the Au particle size increased with calcination temperature, from 3.5 ± 0.9 nm after 400 °C calcination to 11.6 ± 3.1 nm after 700 °C calcination. Based on XRD measurements, calcination also leads to a growth of the rutile TiO_2 particles and a parallel transition of anatase to rutile particles. Pronounced effects occurred, however, only after 700 °C calcination. After calcination, Au was present as metallic nanoparticles (Au^0).

The main results of the kinetic measurements and TAP measurements and the resulting conclusions are as follows:

1. Exposing the calcined or O_2 dosed catalyst to CO pulses results in CO_2 formation, i.e., CO can react with stable oxygen that is reversibly stored on the catalyst surface, and which can be replenished by O_2 pulsing. Hence, gas-phase oxygen is not required for the CO oxidation reaction on these Au/TiO_2 catalysts.
   The amount of stable surface oxygen is constant for a given catalyst and increases about linearly with increasing number of Au perimeter sites, at the perimeter of the interface between the Au nanoparticles and the TiO_2 support. This relation provides strong support for an assignment of these sites as active sites for the adsorption of stable, but nevertheless reactive oxygen.
2. CO is weakly adsorbed and desorbs instantaneously. Pump-probe measurements do not detect any CO_2 formation during an O_2 probe pulse 5 s after a CO pump pulse.
3. Both the kinetic measurements and the single-pulse TAP measurements (simultaneous CO and O_2 pulses) show a distinct decrease in the CO oxidation activity with increasing Au particle

size. Based on the about linear correlation between CO conversion with the number of Au perimeter sites, comparable to that between OSC and number of perimeter sites, we propose that these perimeter sites are the active sites for the CO oxidation reaction and that the reversibly stored oxygen species detected in the multi-pulse experiments represents also the precursor for CO oxidation on the Au/TiO_2 catalyst under present reaction conditions. From the qualitatively similar reaction characteristics in the TAP reactor measurements and in reaction measurements under atmospheric conditions (similar particle size dependence), we suggest that this mechanistic assignment is valid also in the latter case, for reaction under atmospheric pressure.

4. The nature of the active oxygen species cannot be decided upon from the present measurements; atomic or molecular adsorption on the support, however, can be excluded, since these species cannot be formed in the absence of Au nanoparticles, where the OSC and the CO conversion are negligible under present reaction conditions.
5. In multi-pulse experiments, the amount of reversibly removed oxygen is significantly higher in the first sequence of CO pulses, on a freshly calcined Au/TiO_2 catalyst, than that in the second and subsequent ones, while oxygen replenishment is constant in all sequences. Therefore, the amount of strongly adsorbed reactive oxygen is higher after calcination in air at atmospheric pressure than that upon O_2 pulsing. Finally, from the behavior of the CO and CO_2 pulses during the initial phase of the simultaneous CO and O_2 pulses, we conclude that the catalyst undergoes an activation process during this phase based on the apparent CO_2 formation per pulse. Looking at the CO consumption, however, the catalyst deactivates slightly with increasing number of pulses, in contrast to Au/CeO_2, where also the CO consumption increases with increasing number of pulses. The difference between CO_2 formation and CO consumption is attributed to stable CO adsorption in the very initial phase of the CO oxidation reaction, most likely via the formation of surface carbonates. Similar effects are also observed during multi-pulse experiments.
6. The steady-state of the Au/TiO_2 catalyst during CO oxidation is somewhere in between the states obtained after oxidation by calcination or by O_2 pulsing, and that obtained after reduction by CO pulsing. Accordingly, the surface composition of the catalyst surface will sensitively depend on the stoichiometry of the reaction gas mixture. In contrast to Au/CeO_2, the specific surface composition has less effect on the CO oxidation activity.

Acknowledgments

This work was supported by the Deutsche Forschungsgemeinschaft via Priority Programme SPP1181 (Be 1201/13-2). M. Kotobuki is grateful for a fellowship from the Alexander von Humboldt Foundation, D.A. Hansgen for a scholarship from the German Academic Exchange Service (DAAD), respectively. We gratefully acknowledge Dr. A. Chuvilin, L. Kroner and C. Egger (all Ulm University) for the electron microscopy, X-ray diffraction and N_2 adsorption measurements.

Appendix A. Supplementary data

Supplementary data associated with this article can be found, in the online version, at doi:10.1016/j.jcat.2009.03.013.

References

[1] M. Haruta, N. Yamada, T. Kobayashi, S. Iijima, J. Catal. 115 (1989) 301.
[2] F. Boccuzzi, A. Chiorino, J. Phys. Chem. B 104 (2000) 5414.
[3] M. Haruta, CATECH 6 (2002) 102.
[4] M.C. Kung, R.J. Davis, H.H. Kung, J. Phys. Chem. C 111 (2007) 11767.
[5] G.C. Bond, C. Louis, D.T. Thompson, Catalysis by Gold, Imperial Press, London, 2007.
[6] R.M. Finch, N.A. Hodge, G.J. Hutchings, A. Meagher, Q. Pankhurst, M.R.H. Siddiqui, F.E. Wagner, R. Whyman, Phys. Chem. Chem. Phys. 1 (1999) 485.
[7] J. Guzman, B.C. Gates, J. Phys. Chem. B 106 (2002) 7659.
[8] C.K. Costello, M.C. Kung, H.-S. Oh, Y. Wang, H.H. Kung, Appl. Catal. A 232 (2002) 159.
[9] N. Lopez, J.K. Nørskov, J. Am. Chem. Soc. 124 (2002) 11262.
[10] N. Lopez, T.V.W. Janssens, B.S. Clausen, Y. Xu, M. Mavrikakis, T. Bligaard, J.K. Nørskov, J. Catal. 223 (2004) 232.
[11] S.H. Overbury, V. Schwartz, D.R. Mullins, W. Yan, S. Dai, J. Catal. 241 (2006) 56.
[12] M. Mavrikakis, P. Stoltze, J.K. Nørskov, Catal. Lett. 64 (2000) 101.
[13] M. Haruta, Catal. Surv. Jpn. 1 (1997) 61.
[14] M.M. Schubert, S. Hackenberg, A.C. van Veen, M. Muhler, V. Plzak, R.J. Behm, J. Catal. 197 (2001) 113.
[15] L.M. Molina, M.D. Rasmussen, B. Hammer, J. Chem. Phys. 120 (2004) 7673.
[16] F. Boccuzzi, A. Chiorini, Stud. Surf. Sci. Catal. 140 (2001) 77.
[17] J.T. Gleaves, J.R. Ebner, T.C. Kuechler, Catal. Rev. Sci. Eng. 30 (1988) 49.
[18] G.S. Yablonsky, M. Olea, G.B. Marin, J. Catal. 216 (2003) 120.
[19] E.V. Kondratenko, J. Perez-Ramirez, Catal. Today 121 (2007) 159.
[20] J. Perez-Ramirez, E.V. Kondratenko, Catal. Today 121 (2007) 160.
[21] M. Olea, M. Kunitake, T. Shido, Y. Iwasawa, Phys. Chem. Chem. Phys. 3 (2001) 627.
[22] M. Olea, M. Kunitake, T. Shido, K. Asakura, Y. Iwasawa, Bull. Chem. Soc. Jpn. 74 (2001) 255.
[23] M. Olea, Y. Iwasawa, Appl. Catal. A 275 (2004) 35.
[24] M. Olea, M. Tada, Y. Iwasawa, J. Catal. 248 (2007) 60.
[25] M. Olea, M. Tada, Y. Iwasawa, Top. Catal. 44 (2007) 137.
[26] D. Widmann, R. Leppelt, R.J. Behm, J. Catal. 251 (2007) 437.
[27] R. Taha, D. Duprez, N. Mouaddib-Moral, C. Gauthier, Stud. Surf. Sci. Catal. 116 (1998) 549.
[28] C.E. Hori, H. Permana, K.Y. Simon Ng, A. Brenner, K. More, M. Rahmoeller, D. Belton, Appl. Catal. B 16 (1998) 105.
[29] M. Sugiura, Catal. Surv. Asia 7 (2003) 77.
[30] P. Mars, D.W. van Krevelen, Chem. Eng. Sci. 3 (Suppl. 59) (1954) 41.
[31] R. Leppelt, D. Hansgen, D. Widmann, T. Häring, G. Bräth, R.J. Behm, Rev. Sci. Instrum. 78 (2007) 104103.
[32] V. Plzak, J. Garche, R.J. Behm, European Fuel Cell News 10 (2003) 16.
[33] B. Schumacher, V. Plzak, J. Cai, R.J. Behm, Catal. Lett. 101 (2004) 215.
[34] B. Schumacher, Y. Denkwitz, V. Plzak, M. Kinne, R.J. Behm, J. Catal. 224 (2004) 449.
[35] Y. Denkwitz, J. Geserick, U. Hörmann, V. Plzak, U. Kaiser, N. Hüsing, R.J. Behm, Catal. Lett. 119 (2007) 199.
[36] R. Zanella, C. Louis, Catal. Today 107–108 (2005) 768.
[37] M.J. Kahlich, H.A. Gasteiger, R.J. Behm, J. Catal. 171 (1997) 93.
[38] J.T. Gleaves, G.S. Yablonskii, P. Phanawadee, Y. Schuurman, Appl. Catal. A 160 (1997) 55.
[39] G. Bergeret, P. Gallezot, in: G. Ertl, H. Knözinger, J. Weitkamp (Eds.), Handbook of Heterogeneous Catalysis, vol. 2, Wiley-VCH, Weinheim, 1997.
[40] J. Geserick, N. Hüsing, R. Rosmanith, K. Landfester, C.K. Weiss, Y. Denkwitz, R.J. Behm, U. Hörmann, U. Kaiser, Mater. Res. Soc. Symp. Proc., vol. 1007 (Materials Research Society, Boston, 2008), p. S04-13.
[41] M. Haruta, S. Tsubota, T. Kobayashi, H. Kageyama, M.J. Genet, B. Delmon, J. Catal. 144 (1993) 175.
[42] G.R. Bamwenda, S. Tsubota, T. Nakamura, M. Haruta, Catal. Lett. 44 (1997) 83.
[43] M. Haruta, Catal. Today 36 (1997) 153.
[44] M. Valden, X. Lai, D.W. Goodman, Science 281 (1998) 1647.
[45] M.S. Chen, D.W. Goodman, Catal. Today 111 (2006) 22.
[46] N. Lopez, J.K. Nørskov, Surf. Sci. 515 (2002) 175.
[47] J.T. Miller, A.J. Kropf, Y. Zha, J.R. Regalbuto, L. Delannoy, C. Louis, E. Bus, J.A. van Bokhoven, J. Catal. 240 (2006) 222.
[48] M. Haruta, B.S. Uphade, S. Tsubota, A. Miyamoto, Res. Chem. Intermed. 24 (1998) 329.
[49] F. Boccuzzi, A. Chiorino, S. Tsubota, M. Haruta, J. Phys. Chem. 100 (1996) 3625.
[50] H. Liu, A.I. Kozlov, A.P. Kozlova, T. Shido, K. Asakura, Y. Iwasawa, J. Catal. 185 (1999) 252.
[51] S.T. Daniells, A.R. Overweg, M. Makkee, J.A. Moulijn, J. Catal. 230 (2005) 52.
[52] A. Karpenko, R. Leppelt, J. Cai, V. Plzak, A. Chuvilin, U. Kaiser, R.J. Behm, J. Catal. 250 (2006) 139.
[53] Y. Denkwitz, R.J. Behm, unpublished.
[54] Deviations arising from such effects could be avoided or at least reduced by going to lower conversions, e.g., by using lower amounts of catalysts. This is hardly possible, however, in the present case from experimental reasons, since in that case the CO_2 signal for the C700 sample becomes too low.
[55] R.J. Behm, C.R. Brundle, Surf. Sci. 255 (1991) 327.
[56] J.M. Gottfried, K. Christmann, Surf. Sci. 566–568 (2004) 1112.